

Effects of Au Nanoparticles on TiO₂ in the Photocatalytic Degradation of an Azo Dye

Marta Mrowetz¹, Alberto Villa²,
Laura Prati², Elena Selli^{1*}

¹ Dipartimento di Chimica Fisica ed Elettrochimica and CIMAINA, Università degli Studi di Milano, Via Golgi 19, I-20133 Milano, Italy

² Dipartimento di Chimica Inorganica Metallorganica e Analitica and Centro CNR, Università degli Studi di Milano; Via Venezian 21, I-20133 Milano, Italy

* To whom correspondence should be addressed
E-mail: elena.selli@unimi.it

Abstract

The photocatalytic activity of Au modified titanium dioxide was evaluated in the photodegradation of the azo dye Acid Red 1 (AR1) under 254 nm irradiation. Noble metal nanoparticles were deposited on TiO₂ either through deposition-precipitation (DP), or by immobilisation of preformed metallic sols (polyvinylalcohol (PVA)/NaBH₄ or tetrakis(hydroxymethyl)phosphonium chloride (THPC)/NaOH systems). Gold nanoparticles on the photocatalyst surface had dimensions of around 3-4 nm in diameter, as determined by HRTEM analysis, and exhibited visible light plasmon absorption. THPC Au/TiO₂ appears to be the most photoactive amongst the photocatalysts with a 1 wt.% Au loading, while among THPC samples with different Au loadings (0.5-20.0 wt.%) the maximum photoactivity was attained with 5 wt.% Au/TiO₂. The higher AR1 photodegradation rate observed on Au/TiO₂ at basic pH can be related to the higher concentration of hydroxyl anions at the interface: these are able to effectively scavenge photoproduced valence band holes, possibly in competition with Au⁰ oxidation to Au⁺.

Introduction

Photocatalysis on semiconductor oxides has been widely investigated in recent years, mainly because of its high potential for ensuring the complete destruction of organic contaminants both in the aqueous and in the gas phase (1). Titanium dioxide is by far the most extensively studied photocatalytic material, thanks to its outstanding physical properties, high resistance to dark and photoinduced corrosion, easy availability and low cost. Upon photoinduced band gap excitation, electrons are promoted in the semiconductor conduction band and holes are consequently generated in its valence band; such charge carriers are able to reduce and oxidise many species adsorbed on the semiconductor particles and to induce the oxidative destruction of organics up to their overall mineralization, i.e. conversion into CO₂, H₂O and mineral acids. The high rate of recombination between photogenerated electron/hole pairs is a major rate-determining factor controlling photocatalytic efficiency (2).

Noble metal deposition can improve the photocatalytic efficiency of titanium dioxide, by increasing electron/hole separation. For example, small platinum islands deposited on the semiconductor surface have been shown to efficiently compete with the undesired electron-hole recombination reaction, favouring hole trapping and successive oxidation reactions (3). This effect was attributed to electron capture by Pt⁰, rather than to a catalysed oxygen reduction by conduction band electrons (4), i.e. the noble metal deposit can act as a sink for photopromoted electrons (5). In fact, because of the high electronegativity of metal nanoparticles, the Fermi level can be shifted to negative potentials, with a consequent increased accumulation of electrons. Thus, the equilibration of the Fermi-level between the metal itself and the semiconductor favours electron accumulation in the composite metal/TiO₂ system (6).

The deposition of gold nanoparticles on the titanium dioxide surface was explored in the present study as a means of improving its photocatalytic activity. Three different deposition methods were employed, in order to optimize the deposition procedure. In addition to the well-known deposition-precipitation (DP) technique, first used by Haruta (7), the use of metal colloidal solutions was also examined as a way of controlling the size of gold nanoparticles (8), which can affect both the catalytic and photocatalytic performance of Au/TiO₂ systems. The various samples of Au/TiO₂ photocatalysts were evaluated in the photocatalytic degradation of the azo dye Acid Red 1 in the aqueous phase under UV irradiation. The effect of the Au loading on the TiO₂ was also investigated, to maximise the beneficial role of gold on the processes occurring at the water-metal-semiconductor interface. Finally, the effect of pH on the photocatalytic activity of Au/TiO₂ was investigated to ascertain if and how the reactivity of trapped holes at the water-metal-semiconductor interface might be modified by alteration of the photocatalyst surface speciation.

Experimental section

Deposition of gold nanoparticles and

Au/TiO₂ characterisation

Gold foils of 99.9999% purity, purchased from Fluka, poly-vinylalcohol (PVA, 98% hydrolysed, average M_n 13 - 23 x 10³), tetrakis(hydroxymethyl)phosphonium chloride (THPC), purchased either from Fluka or from Aldrich, and TiO₂ from Degussa (P25; 25% rutile, 75% anatase, surface area 50 m² g⁻¹) were used for the preparation of Au/TiO₂ samples. NaOH was 99.9% pure from Merck and was stored under nitrogen.

PVA - stabilised gold sols were obtained from an aqueous solution containing 100 mg l⁻¹ of HAuCl₄, prepared by dissolving 30 mg of gold in a minimum amount of a 3:1 (vol/vol) HCl/HNO₃ mixture. After removing HNO₃, the auric solution was diluted with distilled water and maintained under vigorous stirring while adding a 2 wt.% PVA solution, up to PVA/Au (wt/wt) = 0.64. A 0.1 M freshly prepared NaBH₄ solution was then added up to NaBH₄/Au (mol/mol) = 5, to form a ruby red metallic sol (9).

Sols generated in the presence of the THPC/NaOH system were prepared as reported elsewhere (10). A freshly prepared 0.05 M THPC aqueous solution was added to a 10⁻³ M NaOH solution (THPC/Au (wt/wt) = 0.95). After a few minutes a 10⁻³ M HAuCl₄ solution was added dropwise, forming a brown metallic sol. A reference sample was prepared following exactly the same procedure, apart from HAuCl₄ addition.

The stabilised Au nanoparticles were immobilised on TiO₂ by simply dipping the oxide support in the various metal dispersions, which were acidified up to pH 1.5 - 2 by addition of 6 M H₂SO₄. The amount of TiO₂ powder was calculated so as to have a final gold loading of 1.0 wt.% (PVA Au/TiO₂), or equal to 0.5, 0.7, 1.0, 1.5, 5.0, 7.0, 10 and 20 wt.% (THPC Au/TiO₂). After 1 h the slurry was filtered and the total absorption of gold was checked by ICP analysis of the filtrate. Before use, the photocatalysts were thoroughly washed with distilled water and then dried at 100°C for 2 h.

Alternatively, Au/TiO₂ photocatalyst samples were prepared by the deposition-precipitation (DP) method (7). The TiO₂ support was dispersed in water (approximately 10 ml/g of support) and a 0.3 M NaOH solution was added to raise the pH to 10. The required amount of gold (in the form of HAuCl₄ solution) was added dropwise under vigorous stirring over a time interval of 2 h. The mixture was stirred for 30 min, centrifuged and washed with at least ten times its own volume of distilled water. The reduction of the catalyst was carried out by calcination at 400°C in air for 4 h.

The effect of Au deposition on the crystalline structure of TiO₂ Degussa P25 was analysed by X-ray diffraction employing a Philips PW 1820 powder diffractometer, operating at 40 kV and 40 mA, with Ni-filtered Cu K α radiation (λ = 1.5148 Å). Electron micrographs of the samples were obtained by a Jeol 2000EX microscope, as already reported (11). XPS measurements were performed in an M-Probe Instrument (SSI) equipped with a monochromatic Al-K α source (1486.6 eV) with a 200 x 750 μ m spot size and a 25 eV pass energy.

The Au 4f region around 84 eV was investigated in detail. The accuracy of the reported binding energies can be estimated to be \pm 0.2 eV. A Lambda 19 Perkin-Elmer apparatus, equipped with a RSA-PE-19 accessory for reflectance measurements, was employed to collect DR UV-vis spectra.

Photocatalysis tests

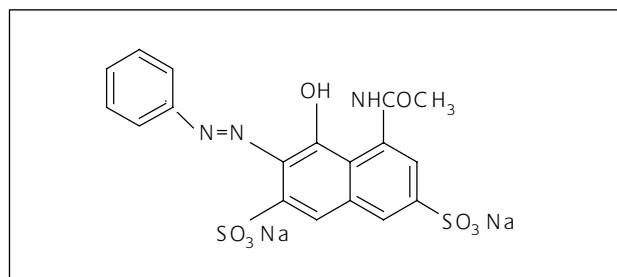
Acid Red 1 (AR1, see Scheme 1) purchased from Aldrich, was purified by repeated crystallisation from methanol and its purity from organic contaminants verified by NMR analysis. All other chemicals used in the photocatalytic experiments were high purity Aldrich products and were employed as received. Water purified by Milli-Q water system (Millipore) was used throughout.

The degradation runs were carried out in the 800 ml reactor previously described (12), equipped with an immersion Jelosil, model NSL15, 15 W low pressure mercury arc lamp, emitting exclusively at 253.7 nm, with a 6.3 x 10⁻⁶ Einstein l⁻¹ s⁻¹ radiation flow, as determined by ferrioxalate actinometry (13). The reactor was magnetically stirred during the runs and thermostated at (30 \pm 1)°C by continuous water recirculation through an external glass jacket.

The irradiated aqueous suspensions contained 0.1 g l⁻¹ of TiO₂ or Au/TiO₂ and an initial AR1 concentration around 2.5 x 10⁻⁵ M. Prior to AR1 addition, the aqueous suspensions containing the photocatalysts were always sonicated for 30 min, employing an ultrasound source emitting at 20 kHz, produced by Stimin (Italy).

The pH of the suspensions was monitored during the photocatalytic runs by means of an Amel Instruments 334-B pH-meter. A pH decrease was observed under so-called natural pH conditions, i.e. when the initial pH of the AR1 aqueous suspensions was not adjusted, from an initial value of 5.8 to a final value of ca. 4.4, as a consequence of the production of stable acids (14). The effect of pH on the rate of AR1 photocatalytic degradation rates was studied by adjusting the initial pH by addition of small amounts of concentrated NaOH and HClO₄ solutions, which are known to have negligible influence on the photocatalytic activity (15).

2-ml samples were periodically withdrawn from the reactors and analysed, after removal of TiO₂ particles by centrifugation at 3000 rpm for 30 min, employing an ALC



Scheme 1

Molecular structure of the azo dye Acid Red 1 (AR1)

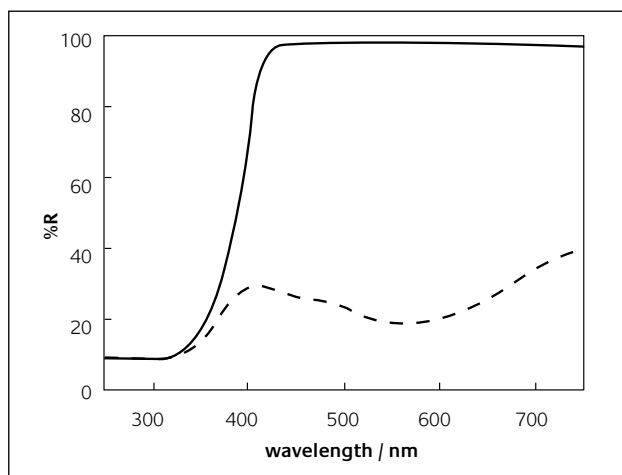


Figure 1
Diffuse reflectance spectra of unmodified TiO_2 (solid line) and 5 wt.% Au/TiO_2 THPC (dashed line)

4225 centrifuge (16). The cleavage of the azo bond of AR1, leading to its bleaching (also mentioned as AR1 degradation), was monitored by spectrophotometric analysis at 531 nm (maximum AR1 absorption, $\epsilon = (3.13 \pm 0.02) \times 10^4 \text{ M}^{-1} \text{ cm}^{-1}$) by means of a Perkin Elmer Lambda 16 spectrophotometer (16). The mineralisation of the substrate was detected using a total organic carbon (TOC) analyser (Shimadzu Instruments, TOC-5000A). All runs were repeated at least twice, to check their reproducibility.

AR1 adsorption was determined in aqueous suspensions containing 1.0 g l^{-1} of TiO_2 or Au modified TiO_2 and a $2.5 \times 10^{-5} \text{ M}$ initial AR1 concentration. After continuous stirring for 24 h in the dark at 30°C , the photocatalyst was removed by centrifugation and the aqueous phase was analysed spectrophotometrically for AR1 residual content.

Results and discussion

Photocatalysts characterisation

Deposition-precipitation (DP) and two quite novel methods, employed for the first time to prepare Au/TiO_2 photocatalysts (17-21) and based on the reduction of HAuCl_4 , either with NaBH_4 in the presence of polyvinylalcohol (PVA) (11) or with the tetrakis(hydroxymethyl)phosponium chloride (THPC)/NaOH system (8), were employed to deposit gold nanoparticles on the surface of titanium dioxide.

The deposition of gold nanoparticles on TiO_2 was confirmed by the colour change of the modified oxide powder, turning from white into deep purple, a colour deriving from the surface plasmon resonance of Au^0 islands (22). In fact, the diffuse reflectance UV-vis spectra of unmodified TiO_2 and of 5 wt.% Au/TiO_2 THPC shown in Figure 1 indicate that, while unmodified titanium dioxide reflects strongly at wavelengths above 400 nm, Au-modified TiO_2 exhibits a less evident absorption edge at 400 nm, followed by the plasmon resonance absorption of Au nanoparticles at longer wavelengths. Light absorption by the deposited metal causes a collective oscillation of the

Table 1: Comparison between 1 wt.% Au/TiO_2 prepared by the DP, PVA and THPC method: diameter of gold nanoparticles, measured by HRTEM analysis, and first order rate constants of AR1 photocatalytic degradation

Sample	d_{Au} (HRTEM) / nm	$10^4 \times k / \text{s}^{-1}$
THPC	3.6	7.0 ± 0.7
PVA	3.5	6.4 ± 0.3
DP	4.2	6.0 ± 0.2

free conduction band electrons of the gold nanoparticles as a consequence of their optical excitation (23), a phenomenon observed when the wavelength of the incident light far exceeds the particle diameter (24). The plasmon resonance, responsible for absorption in the visible region, does not induce any photocatalytic activity of Au/TiO_2 under visible light irradiation (21), because no holes are photoproduced in the semiconductor valence band under absorption by the metal nanoparticles deposited on the TiO_2 surface.

Figure 2 shows the XRD patterns of unmodified TiO_2 and of 1.0, 5.0 and 20 wt.% Au/TiO_2 THPC samples. Gold deposition did not affect the anatase and rutile phases, which can be easily distinguished by the peaks at $ca. 2\theta = 25.4^\circ$ and 27.5° , respectively. The THPC as well as the PVA methods implied gold deposition on TiO_2 at room temperature and this guarantees the persistence of the optimal anatase to rutile ratio of Degussa P25, without any structural modification induced by thermal treatment. Au deposition was responsible for new peaks typical of crystalline gold at $ca. 2\theta = 38.5^\circ$ and 44° (25). Their intensity increased with Au loading, the Au phase being hardly detectable in 1 wt.% Au, as previously reported (26).

High resolution XPS spectra of the Au(4f) region of the 1 wt.% Au/TiO_2 THPC sample, recorded before and after 3 h irradiation at 254 nm, are given in Figure 3. They exhibit two peaks at binding energies (BE) of $ca. 83.6 \text{ eV}$ and 87.3 eV , originating from $\text{Au } 4f_{7/2}$ and $\text{Au } 4f_{5/2}$ electrons of Au(0),

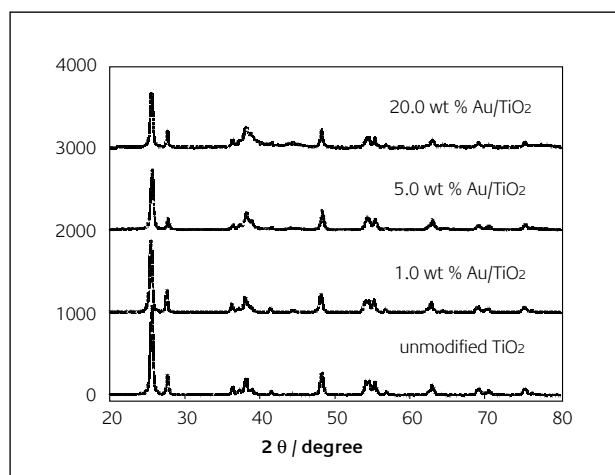


Figure 2
XRD patterns of unmodified TiO_2 and of 1 wt.%, 5 wt.% and 20 wt.% Au/TiO_2 THPC

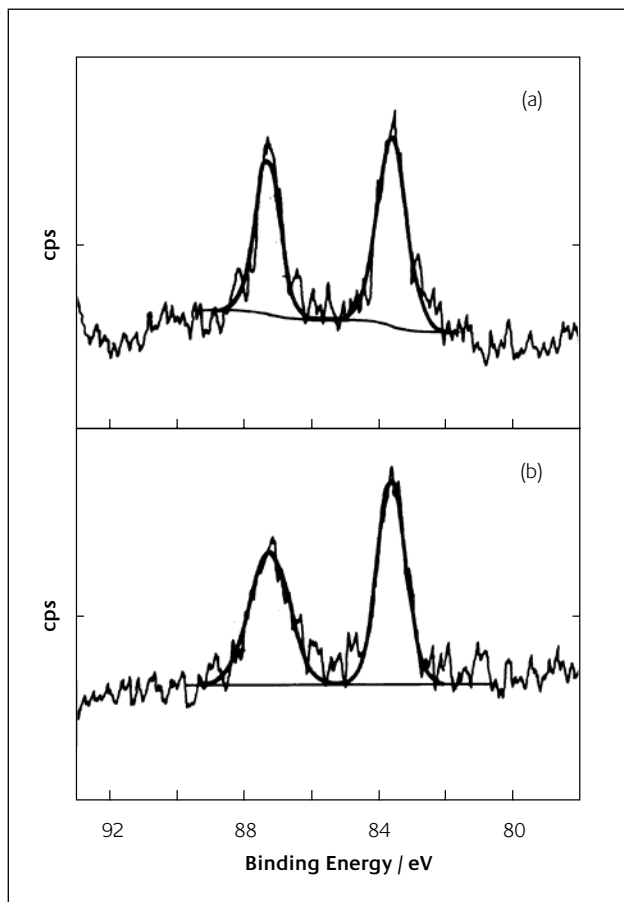


Figure 3
High resolution XPS scan of the Au (4f) region of 1 wt.% Au/TiO₂ THPC (a) before irradiation and (b) after 3 h irradiation at 254 nm

respectively. Similar spectra have been recently reported for THPC Au/TiO₂ samples, also exhibiting a shift to lower BE compared to the Au reference (26). This has been attributed to the increased fraction of surface atoms, which, being less coordinated, exhibit reduced screening of the photoelectron core hole. The small change in the peaks shape noticed after irradiation (Figure 3) might be ascribed to the presence of oxidised Au forms, as in similar Au/TiO₂ systems (27,28). In fact, although most of the photogenerated holes are generally scavenged by surface hydroxyl groups, a fraction of them can react with metallic gold on the photocatalyst surface, converting it into Au(I) and possibly then into Au(III), the oxidation potential of the holes photogenerated in the semiconductor valence band ($E_{vb} \sim 2.5$ V) being more positive than that of metallic gold ($E^{\circ}(\text{Au}/\text{Au}^+) = 1.76$ V) (5).

The effect of gold deposition was also examined by HRTEM analysis, yielding information on the dimension and the distribution of the Au nanoparticles on the TiO₂ surface. As reported in Table 1, the mean diameter of gold nanoparticles in 1 wt.% Au/TiO₂ varied between 3.5 and 4.2 nm, depending on the preparation procedure, in agreement with previous results for similar Au loadings (29). The preparative methods employed using Au sols as starting materials guarantee the maintenance of Au particle size in the deposition step on the TiO₂ surface, as already verified on different supports (11).

Photocatalytic activity

Preliminary tests, performed to verify if gold nanoparticles affect AR1 adsorption on the semiconductor, revealed that ca. 28% of the azo dye (2.5×10^{-5} M) was adsorbed on the unmodified titanium dioxide surface (1.0 g l^{-1}) and only ca. 17% on the Au modified surface (1.0 g l^{-1} of the 1 wt.% Au/TiO₂ DP sample). The iso-electric point of Au-modified TiO₂ has been reported to shift to lower pH values (17) with respect to unmodified TiO₂, thus extending the pH region where the photocatalyst surface is negatively charged. Of course this inhibits the adsorption of negatively charged compounds, such as the bisulfonic azo dye AR1. Moreover, Au deposition can also alter TiO₂ surface speciation. Recent DRIFTS studies indicated a substantial decrease of the surface amount of -OH groups in the presence of nanoscopic gold particles, especially for high Au loadings (21).

In order to identify the most suitable Au deposition method for the preparation of efficient Au/TiO₂ photocatalysts, the activity of the various 1 wt.% Au/TiO₂ samples, prepared using the different methods, was first compared. Prior to their use as photocatalysts, all PVA and THPC samples underwent a pre-treatment step, consisting in a 3 h - long pre-irradiation at 254 nm of their water suspensions in the absence of substrate. In this way, the gold nanoparticle stabilisers, i.e. polyvinylalcohol or tetrakis(hydroxymethyl)phosphonium chloride, could be efficiently removed photocatalytically. Indeed, both types of Au/TiO₂ photocatalysts exhibited a much lower activity in AR1 photocatalytic degradation if they were employed without any pre-treatment (see for example Figure 4). Longer pre-irradiation did not improve the photocatalytic activity of PVA and THPC samples. By contrast, DP samples did not require any pre-irradiation treatment, no organics having been used in their preparation. Indeed, AR1 photodegradation on pre-irradiated DP Au/TiO₂ proceeded at exactly the same rate as on not pre-treated DP Au/TiO₂ (Figure 4).

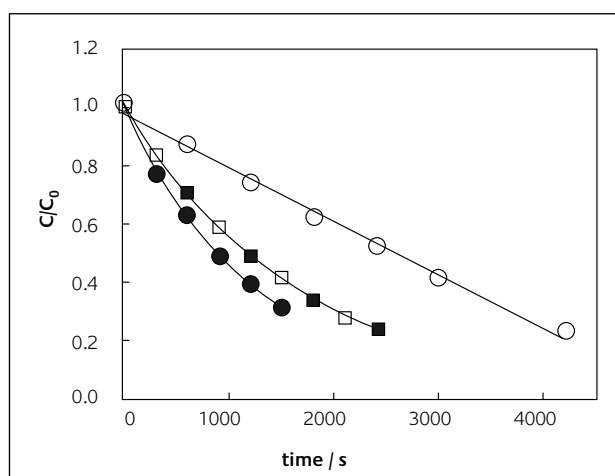


Figure 4
Effect of 3 h - long pre-irradiation at 254 nm of Au/TiO₂ (1 wt.%) on AR1 photocatalytic degradation: DP (squares) and THPC (circles) as synthesised (open symbols) and after 3 h - long pre-irradiation (full symbols)

The first order rate constants of AR1 photocatalytic degradation reported in Table 1 indicate THPC Au/TiO₂ as the best performing photocatalyst, with the PVA and DP photocatalyst samples being progressively less efficient, in that order. Most probably, the lower activity of DP compared to THPC and PVA Au/TiO₂ is derived from the calcination step at 400°C, required for reducing Au(III) to Au(0) only in the DP preparation route. Calcination not only reduces the surface area and the quantity of OH surface groups, but, in the case of TiO₂, may also induce some conversion of the anatase phase into the rutile phase, which might be less photoactive (1). Moreover, heat treatment may also increase the gold particles size (30). Indeed, the rate constant of AR1 photodegradation on a PVA Au/TiO₂ sample, which had been calcined at 400°C, was *ca.* 25% lower than that obtained employing a non calcined PVA sample.

The effect of the Au loading, deposited on the TiO₂ surface through the most efficient THPC method, was investigated in the 0.5 – 20 wt.% Au/TiO₂ range. The first order rate constants of AR1 photocatalytic degradation are collected in Table 2. An increase of the photocatalytic efficiency was obtained by increasing the amount of gold up to 5 wt.%; and in this range the rate constants of AR1 photodegradation were equal to (0.5 wt.% Au/TiO₂) or higher (0.7, 1.0 and 5.0 wt.% Au/TiO₂) than that obtained on titanium dioxide containing no gold. Thus, low gold loadings are not very effective in reducing the rate of recombination between the conduction band electrons and the valence band holes and a substantial increase of photoactivity can be attained for Au loadings above 1 wt.%. In contrast, very high Au loadings, e.g. 20 wt.% Au on TiO₂, had a negative effect on the photodegradation rate, mainly due to lower substrate adsorption on the oxide surface and to screening effects, with the metal deposits reducing the direct absorption of light by titanium dioxide and thus the photogeneration of charged species. Moreover, Au

Table 2: Effect of Au loading of Au/TiO₂ THPC photocatalysts on the first order rate constants of AR1 photocatalytic degradation

Au loading / wt.%	10 ⁴ × k / s ⁻¹
0	5.8 ± 0.5
0.5	5.6 ± 0.2
0.7	6.2 ± 0.5
1.0	7.0 ± 0.7
5.0	8.6 ± 0.6
20	3.7 ± 0.3

nanoparticles can also act as effective scavengers of photogenerated holes (*vide infra*), inhibiting their reaction with the substrate (19).

The photocatalytic degradation of organic water pollutants, such as AR1, notoriously produces intermediate species, whose toxicity may be higher than that of the starting compound. Thus, the extent of mineralization, i.e. the effective conversion of organic compounds into CO₂, H₂O and mineral acids, should always be checked. Figure 5 gives the AR1 photomineralization profiles in unmodified TiO₂ and in 1 and 5 wt.% Au/TiO₂ THPC suspensions, as monitored by total organic carbon (TOC) analysis. Of course, AR1 photomineralization proceeded at a much lower rate than AR1 photodegradation; in fact, as shown in Figure 5, a 50% reduction of the TOC content was attained after a *ca.* 5-fold longer irradiation time, respect to the irradiation time required to halve the AR1 initial concentration. On the other hand, the Au loading of TiO₂ had the same effect in AR1 photodegradation and photomineralization, this latter proceeding on 5 wt.% Au/TiO₂ at a higher rate than on 1 wt.% Au/TiO₂, which behaved only slightly better than unmodified TiO₂. Thus, the beneficial effect of Au nanoparticles deposition on TiO₂ is not specific for the photocatalytic degradation of AR1, but it was confirmed

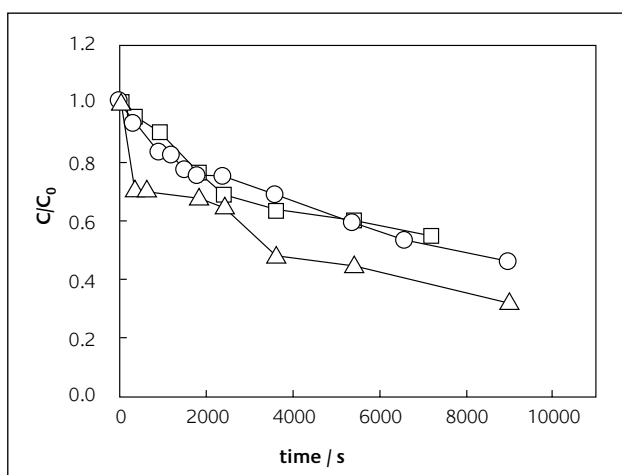


Figure 5
Effect of Au loading on the photocatalytic mineralization of AR1: unmodified TiO₂ (squares), 1 wt.% (circles) and 5 wt.% (triangles) Au/TiO₂ THPC

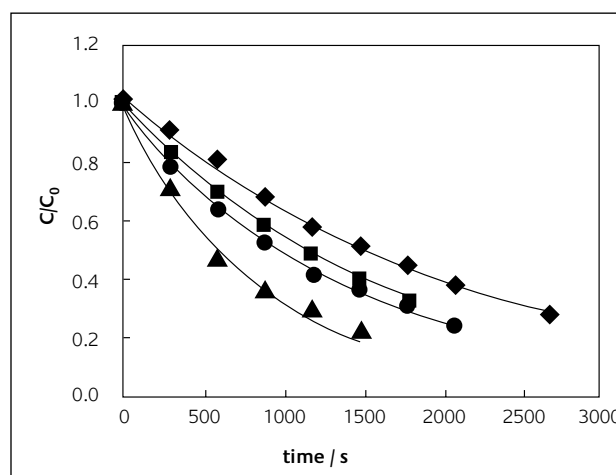


Figure 6
Effect of pH on AR1 photocatalytic degradation in 1 wt.% Au/TiO₂ THPC suspensions: pH 3 (diamonds), pH 4 (squares), natural pH (circles) and pH 9.6 (triangles)

also for the photocatalytic degradation of its mineralization by-products.

Finally, the effect of pH on the rate of AR1 photocatalytic degradation was also investigated in the presence of 1 wt.% Au/TiO₂ THPC. The results obtained in the 3 – 10 pH range, given in Figure 6, should be considered in comparison with the pH-dependence of the rate of AR1 photocatalytic degradation on unmodified TiO₂, exhibiting a maximum under so-called natural pH conditions (31), i.e. for an initial pH of 5.8, corresponding to optimal conditions for electrostatic interaction between the negatively charged AR1 molecule and the positively charged TiO₂ surface. Lower rates were measured under 254 nm irradiation either at lower or at higher pH, the rate constant of AR1 photocatalytic degradation on TiO₂ at pH 9.6 being more than 20% lower than that measured at natural pH, in line with the results of AR1 photocatalytic degradation on TiO₂ under longer wavelength irradiation (31). Surprisingly, AR1 photodegradation on Au/TiO₂ proceeded significantly faster at pH 9.6 (Figure 6), i.e. the photocatalytic activity of Au-modified titanium dioxide increases with increasing the OH⁻ concentration in the aqueous phase.

There is indirect evidence of a reaction occurring between the surface metallic gold and the valence band holes. In fact, in the presence of a high concentration of hydroxide, hydroxyl radicals can be generated more easily by reaction with valence band holes (32). Under such conditions the hydroxide anions in the aqueous phase can compensate for the smaller concentration of hydroxyl groups on the Au modified surface (21) and act as effective scavengers for photoproducted holes. Thus, the higher photocatalytic degradation rates obtained under these conditions are a consequence of the lower probability that valence band holes oxidise Au⁰ to Au⁺, which will act as a recombination centre, in contact with conduction band electrons. The beneficial effect of gold deposition on TiO₂ thus seems to be strictly related to the minimisation of the reaction between metallic Au and photogenerated holes.

Conclusions

The deposition of nanosized gold particles on the TiO₂ surface may increase the photocatalytic activity of the semiconductor oxide, by increasing the efficiency of charge separation of the light-generated electron-hole pairs. The best photocatalytic activity was attained with THPC Au/TiO₂, after a pre-irradiation step to remove the colloidal stabiliser. Optimal Au loadings should be employed (5 wt.% Au on TiO₂ in the present case), possibly depending on the adsorption properties of the substrate, for ensuring optimal charge separation without excessive light screening effects of the TiO₂ particles.

About the authors



Marta Mrowetz graduated in Chemistry (2002) and completed her PhD in Chemical Sciences (2006) at the University of Milan under the supervision of Prof. E. Selli. In 2004 she spent several months at Caltech, working with A.J. Colussi and M.R. Hoffmann. Then she was awarded a post-doc position at the University of Milan. She has always been involved in the mechanistic aspects of photocatalysis on semiconductors.



Alberto Villa presently works as a PhD student in the laboratory of Prof. Laura Prati in the Inorganic Chemistry Department at the University of Milan. He is a graduate in Industrial Chemistry (2004), his main interest being in catalytic oxidation reactions. The particular experience he has acquired is in the field of preparation of gold on carbon and its use in liquid phase oxidation.



Laura Prati is presently an Associate Professor in Inorganic Chemistry at the University of Milan. She is a graduate in Chemistry (1983), received her specialisation in “Tecniche Analitiche per la Chimica Organica Fine” from Politecnico of Milan in 1985 and was awarded a PhD in Industrial Chemistry in 1988. Her main interest is in catalytic hydrogenation and oxidation reactions and she has been involved in catalytic applications for gold since 1986. Particular experience she had acquired is in the field of preparation of gold on carbon and its use in the liquid phase oxidation.



Elena Selli graduated in Chemistry at the Scuola Normale Superiore in Pisa (Italy) in 1977. She has been a PhD student and research fellow of the Scuola Normale Superiore (1981) and of the University of Milan (1983). She is now an associate professor of physical chemistry at the University of Milan. She has always been involved in mechanistic studies of photoreactions. In recent years, her interests were mainly focused on electron transfer processes occurring in photocatalytic processes on semiconductors, for both water purification and energy storage.

References

- 1 M. R. Hoffmann, S.T. Martin, W. Choi and D.W. Bahnemann, *Chem. Rev.*, 1995, **95**, 69
- 2 A. L. Linsebigler, G. Lu and J.T. Yates, Jr., *Chem. Rev.*, 1995, **95**, 735
- 3 F. B. Li and X.Z. Li, *Chemosphere*, 2002, **48**, 1103
- 4 Z. Kasarevic-Popovic, D. Behar and J. Rabani, *J. Phys. Chem. B*, 2004, **108**, 20291

- 5 V. Subramanian, E. E. Wolf and P.V. Kamat, *J. Phys. Chem. B*, 2001, **105**, 11439; *Langmuir*, 2003, **19**, 469
- 6 A. Wood, M. Giersig and P. Mulvaney, *J. Phys. Chem. B*, 2001, **105**, 8810
- 7 M. Haruta, *Catal. Today*, 1997, **36**, 153
- 8 J.-D. Grunwaldt, C. Kiener, C. Wögerbauer and A. Baiker, *J. Catal.*, 1999, **181**, 223
- 9 L. Prati and G. Martra, *Gold Bull.*, 1999, **32**, 96
- 10 D. G. Duff, A. Baiker and P. Edwards, *J. Chem. Soc., Chem. Commun.*, 1993, 96
- 11 F. Porta, L. Prati, M. Rossi, S. Coluccia and G. Martra, *Catal. Today*, 2000, **61**, 165
- 12 M. Bertelli and E. Selli, *Appl. Catal. B: Environ.*, 2004, **52**, 205
- 13 C. G. Hatchard and C.A. Parker, *Proc. R. Soc. London*, 1956, **A235**, 518
- 14 J. M. Joseph, H. Destailats, H.M. Hung and M.R. Hoffmann, *J. Phys. Chem. A*, 2000, **104**, 301
- 15 M. Abdullah, J.K.C. Low and R.W. Matthews, *J. Phys. Chem.*, 1990, **94**, 6820
- 16 M. Mrowetz, C. Pirola and E. Selli, *Ultrason. Sonochem.*, 2003, **10**, 247
- 17 X. Z. Li and F.B. Li, *Environ. Sci. Technol.*, 2001, **35**, 2381
- 18 I. M. Arabatzis, T. Stergiopoulos, D. Andreeva, S. Kitova, S.G. Neophytides and P. Falaras, *J. Catal.*, 2003, **220**, 127
- 19 A. Dobosz and A. Sobczynski, *Monatsh. Chem.*, 2001, **132**, 1037
- 20 S. Sakthivel, M. V. Shankar, M. Palanichamy, B. Arabindoo, D.W. Bahnemann and V. Murugesan, *Water Res.*, 2004, **38**, 3001
- 21 A. Orlov, D.A. Jefferson, N. Macleod and R. M. Lambert, *Catal. Letters*, 2004, **92**, 41
- 22 U. Kreibig and M. Vollmer, *Optical Properties of Metal Clusters*; Springer-Verlag: Berlin, 1995
- 23 M. M. Alvarez, J. T. Khoury, T. G. Schaaff, M. N. Shafigullin, I. Vezmar and R. L. Whetten, *J. Phys. Chem. B*, 1997, **101**, 3706
- 24 P. V. Kamat, *J. Phys. Chem. B*, 2002, **106**, 7729
- 25 A. Watanabe and H. Kozuka, *J. Phys. Chem. B*, 2003, **107**, 12713
- 26 X. Z. Li, C. He, N. Graham and Y. Xiong, *J. Appl. Electrochem.*, 2005, **35**, 741
- 27 A. Zwijnenburg, A. Goossens, W. G. Sloof, M. W. J. Crajé, A. M. van der Kraan, L. Jos de Jongh, M. Makkee and J.A. Moulijn, *J. Phys. Chem. B*, 2002, **106**, 9853
- 28 M. P. Casaletto, A. Longo, A. Martorana, A. Prestianni and A. M. Venezia, *Surf. Interface Anal.*, 2006, **38**, 215
- 29 T. Hayashi, K. Tanaka and M. Haruta, *J. Catal.*, 1998, **178**, 566
- 30 A. G. Shastri, A. K. Datye and J. Schwank, *J. Catal.*, 1984, **87**, 265
- 31 M. Mrowetz and E. Selli, *J. Photochem. Photobiol. A: Chem.*, 2006, **180**, 15
- 32 I. K. Konstantinou and T. A. Albanis, *Appl. Catal. B: Environ.*, 2004, **49**, 1